

The dimension of loop-erased random walk in 3D

David B. Wilson

Microsoft Research, Redmond, WA 98052, USA

(Dated: August 6, 2010; revised October 7, 2010)

We measure the fractal dimension of loop-erased random walk (LERW) in 3 dimensions, and estimate that it is 1.62400 ± 0.00005 . LERW is closely related to the uniform spanning tree and the abelian sandpile model. We simulated LERW on both the cubic and face-centered cubic lattices; the corrections to scaling are slightly smaller for the face-centered cubic lattice.

INTRODUCTION

Loop-erased random walk (LERW) is the path obtained from a random walk by erasing loops as they are formed, and was introduced by Lawler. The paths connecting points in a uniformly random spanning tree are distributed as loop-erased random walk [1–3]. Uniform spanning trees in turn are closely related to the abelian sandpile model of self-organized criticality [4], and properties of loop-erased random walk manifest themselves in the avalanches of these sandpiles. In particular, the fractal dimension z of LERW is related to the scaling behavior of topplings in the sandpile models [5, 6].

In two dimensions, LERW has dimension $5/4$ [1, 7, 8], and its scaling limit (with suitable boundary conditions) is known to be SLE_2 [9]. In dimensions 4 and higher, LERW has dimension 2, though with a cube-root log correction in 4D [10]. In dimension 5 and higher, the scaling limit of LERW is Brownian motion. By contrast, relatively little is known about LERW in 3D.

Kozma proved that 3D LERW (in certain domains) has a scaling limit that is invariant under rotations and dilations [11]. The Hausdorff dimension of 3D LERW is not rigorously known to be well-defined, but $1 < z \leq 5/3$ [12]. There have been a number of estimates of this dimension z , sometimes expressed in terms of $\nu = 1/z$ or 2ν . Guttmann and Bursill estimated $2\nu = 1.600 \pm 0.006$ in $d = 2$ and $2\nu = 1.232 \pm 0.008$ in $d = 3$ [13]. Bradley and Windwer estimated $2\nu = 1.571 \pm 0.006$ in $d = 2$ and $2\nu = 1.230 \pm 0.003$ in $d = 3$ [14]. Anton predicted $\nu = 8/13$ exactly [15]. Agrawal and Dhar estimated $z(d = 3) = 1.6183 \pm 0.0004$ [16]. Fedorenko, Le Doussal, and Wiese gave an expansion for spatial dimension $4 - \varepsilon$:

$$z(d = 4 - \varepsilon) = 2 - \frac{\varepsilon}{3} - \frac{\varepsilon^2}{9} + O(\varepsilon^3).$$

Evaluating this series at $\varepsilon = 1$, they estimated $z(d = 3) = 1.614 \pm 0.011$ [17]. More recently, Grassberger estimated $z(d = 3) = 1.6236 \pm 0.0004$ [18], contradicting Agrawal and Dhar’s earlier estimate. Our estimate is even more precise: 1.62400 ± 0.00005 . These estimates are summarized in Table I.

dimension of 3D LERW	reference
$1 < z \leq 5/3$ (rigorous)	Lawler [12]
1.623 ± 0.01	Guttmann & Bursill [13]
1.626 ± 0.004	Bradley & Windwer [14]
$13/8$ (conjectured exact)	Anton [15]
1.6183 ± 0.0004	Agrawal & Dhar [16]
1.614 ± 0.011	Fedorenko, Le Doussal, & Wiese [17]
1.6236 ± 0.0004	Grassberger [18]
1.62400 ± 0.00005	present work

TABLE I: Estimates of the dimension z of loop-erased random walk in 3 dimensions.

SIMULATION DESIGN

Most earlier simulations (with the exception of Agrawal and Dhar’s simulations [16]) look at the length of the loop erasure of a random walk run for a large number of time steps. The starting point of a loop-erased random walk has different statistical properties than typical points on the LERW path. For example, the winding angle variance at the starting point of LERW is different than at a typical point [19, 20]. To measure the dimension of LERW, we would like to measure the length of an LERW path without the atypical starting point.

Agrawal and Dhar’s simulations instead created loop-erased random loops, and measured their lengths. Dhar and Dhar had argued that adding an edge to a tree creates a loop of size ℓ with probability $\approx \ell^{-2/z}$, and that the next step of an LERW produces a loop of size ℓ with probability $\approx \ell^{-1-2/z}$ [21]. Agrawal and Dhar estimated the LERW dimension z by looking at the sizes of these erased loops. In their estimate, it was necessary to ignore both small loops (because of lattice effects) and large loops (which were influenced by the LERW stopping condition), effectively leaving fewer length scales with which to estimate the dimension.

In our simulations, we ran a random walk on an $L \times L \times L$ torus while erasing contractible loops, until a noncontractible loop-erased random loop was formed, and reported its length. This random variable is equidistributed to the following: Generate a uniformly random directed subgraph of the torus, where each vertex has

out-degree 1, conditioned on there being no contractible cycles. Every vertex leads to a cycle that winds around the torus. Pick a random vertex, find the cycle that it leads into, and report its length. By taking many such measurements for different L 's, we estimated the dimension of LERW.

The geometry of the torus affects the length distribution of the noncontractible loop, but for different L 's the effect is the same. While Agrawal and Dhar had to ignore both small loops and large loops, we only need to ignore the small L 's (because of lattice effects), so it is easier to see the asymptotic behavior.

CHOICE OF LATTICE

Kozma proved that LERW on any 3D lattice converges to the same scaling limit [11], which is invariant under dilations and rotations, provided that random walk on the lattice converges to Brownian motion. To measure the dimension or other properties of LERW, in addition to using the standard cubic lattice, we also tried the face-centered cubic (FCC) lattice. The FCC lattice arises from the densest packing of spheres in 3D. Each site is adjacent to 12 nearest neighbors, as opposed to 6 nearest neighbors in the cubic lattice. In this sense the FCC lattice is closer to being isotropic than the cubic lattice, and since the scaling limit of LERW is isotropic, we might expect that LERW on the FCC lattice behaves more like the isotropic scaling limit for smaller values of L than LERW on the cubic lattice.

The most convenient way to simulate on the face-centered cubic lattice is to use the same $L \times L \times L$ grid as for the cubic lattice, but with extra edges, where x and y are connected if $x - y$ is one of $(\pm 1, 0, 0)$, $(0, \pm 1, 0)$, $(0, 0, \pm 1)$, $(\pm 1, \mp 1, 0)$, $(0, \pm 1, \mp 1)$, or $(\pm 1, 0, \mp 1)$. In addition to changing the lattice, this also changes the geometry of the torus, making it a skew torus. But the geometry of this skew torus is plausibly better than the geometry of the ordinary torus, since the girth divided by volume^{1/3} is larger.

Our simulations suggest that the face-centered cubic lattice gives slightly better results than the ordinary cubic lattice for systems with the same side length L . It would be interesting to see what effect the choice of lattice has on simulations in higher dimensions, where there are lattices that are much better (by some measures) than the hypercubic lattice.

LOOP HOMOLOGY

In order for the measured loop length to be related to the dimension of LERW, we would need to know that the loops do not wind around the torus too many times, and in particular that the number of windings does not

	homology	$L = 64$	$L = 1024$	$L = 16384$
cubic lattice cubic torus	1,0,0	0.6242	0.6214	0.6212
	1,1,0	0.2804	0.2813	0.2814
	1,1,1	0.0613	0.0618	0.0619
	2,1,0	0.0163	0.0169	0.0170
	2,1,1	0.0084	0.0087	0.0087
	2,0,0	0.0077	0.0080	0.0080
	2,2,1	0.0007	0.0007	0.0007
	2,2,0	0.0005	0.0006	0.0006
	3,1,0	0.0002	0.0002	0.0002
	3,1,1	0.0001	0.0001	0.0001
	3,0,0	0.0001	0.0001	0.0001
FCC lattice skew torus	1, 0, 0	0.8395	0.8377	0.8375
	1, 1, -1	0.0781	0.0784	0.0785
	1, 1, 0	0.0674	0.0683	0.0684
	2, 0, 0	0.0067	0.0070	0.0070
	2, 1, -1	0.0061	0.0063	0.0063
	2, 1, 0	0.0012	0.0013	0.0013
	1, 1, 1	0.0007	0.0007	0.0008
	2, 2, -1	0.0001	0.0001	0.0001
	2, 2, -2	0.0001	0.0001	0.0001

TABLE II: Empirical probability distribution of the homology (up to symmetry) of the noncontractible loop.

grow with the side length L (as it would in 5 and higher dimensions). Therefore we measured the homology of the noncontractible loop in addition to its length, and found that in fact it does not grow with L (see Table II).

The fact that the loops with high probability do not wind around the torus more than $O(1)$ times can be deduced as follows. A classical result says that two independent random walks started distance R apart and run R^2 steps in \mathbb{Z}^3 have a constant chance of intersecting. Lyons, Peres, and Schramm [22] showed that whenever two independent random walks intersect with constant probability, the second random walk intersects the loop-erasure of the first with constant probability. Every time the random walk winds twice more around the $L \times L \times L$ torus, there is a constant chance that the second time around it intersects the loop-erasure of the first time around. So the number of windings is stochastically dominated by a geometric random variable, uniformly in L .

NOTES ON THE SIMULATIONS

We collected an enormous amount of data (using high performance computing clusters), e.g., 10^9 data points for $L = 16384$ for two different lattices, where each data point requires $\approx L^2$ random walk steps, for a total of $\approx 5 \times 10^{17}$ random walk steps. For the results to be meaningful, we require a high-quality random number generator, and we used one based on the advanced encryption standard (AES-256), which has been found to have excellent statistical properties [23, 24].

lattice	$2^8, \dots, 2^{14}$	$2^9, \dots, 2^{14}$	$2^{10}, \dots, 2^{14}$	$2^{11}, \dots, 2^{14}$	$2^{12}, \dots, 2^{14}$	$2^{13}, 2^{14}$
cubic	$1.62393 \pm .00001$ $0.11712 \pm .00006$ $p = 3 \times 10^{-22}$	$1.62396 \pm .00001$ $0.11687 \pm .00008$ $p = 0.03$	$1.62397 \pm .00001$ $0.11677 \pm .00011$ $p = 0.4$	$1.62398 \pm .00002$ $0.11668 \pm .00015$ $p = 0.75$	$1.62398 \pm .00003$ $0.1167 \pm .0003$ $p = 0.57$	$1.62399 \pm .00006$ $0.1166 \pm .0005$ p undefined
	FCC	$1.62394 \pm .00001$ $0.09081 \pm .00006$ $p = 3 \times 10^{-13}$	$1.62396 \pm .00001$ $0.09062 \pm .00007$ $p = 0.08$	$1.62397 \pm .00001$ $0.09054 \pm .00010$ $p = 0.41$	$1.62398 \pm .00002$ $0.09048 \pm .00015$ $p = 0.43$	$1.62399 \pm .00003$ $0.0904 \pm .0002$ $p = 0.56$

TABLE III: Estimates of the 3D LERW dimension from the data. Different sets of system size L were used; the fit in the first data column was for $L \in \{2^8, 2^9, 2^{10}, 2^{11}, 2^{12}, 2^{13}, 2^{14}\}$, while the last column used only $L \in \{2^{13}, 2^{14}\}$. The fits shown here are least-squares fits of $\log(\mathbb{E}[\text{loop length}])$ to functions of the form $z \log L + a$, where we used 10^9 data points for each system size L . (The parameter a depends upon the lattice, but z is the same for both lattices.) The error bars given are the 95% confidence intervals (± 1.96 standard deviations) of the fitted parameters (z and a). For each such fit we did a χ^2 test, and give the p -value of the χ^2 statistic.

Following Agrawal and Dhar [16], we used a hashtable of points visited by the loop-erased random walk to identify newly created loops. The storage requirements are then order $L^{1.6240\dots}$ rather than order L^3 . However, unlike the hashtables in other simulations [16, 18], rather than use linked lists in the event that two different points on the LERW accidentally hash to the same entry in the hashtable, we used an “open address” hash table, since they have less data structure overhead [25]. Open address hash tables are not normally suitable when entries can be deleted (such as when loops are erased), but in the case of LERW simulations, we may delete the points in an erased loop in reverse chronological order, and in this case open addressing works with deletions.

ESTIMATE OF DIMENSION

Table III summarizes some simple least-squares fits of the data to estimate the dimension, which suggest an exponent of 1.6240. In Fig. 1 we show our simulation data for the length of the noncontractible loop in a histogram type format. It is evident from this figure that the exponent 1.6240 is at least approximately correct.

To estimate the exponent to four decimals from a plot, we need another way to present the data. Therefore we let $Q_q(L)$ denote the q^{th} quantile for loop length on a system of size L . For example, $Q_{0.5}(16384)$ is the empirical median loop length for the torus of order 16384. For any q , we would expect $Q_q(L)$ to take the form $a(q)L^z$ for large L . More precisely, we would expect there to be a correction term, most likely of the form $Q_q(L) = a(q)L^z + b(q)L^y + \dots$, where y might be related to the exponent for a close encounter of the LERW path with itself. Then

$$\frac{\log(Q_q(L_1)/Q_q(L_2))}{\log(L_1/L_2)} = z + \frac{b(q)/a(q)}{\log(L_1/L_2)} (L_1^{y-z} - L_2^{y-z}) + \dots$$

In Fig. 2, we plot these ratios of empirical quantiles to estimate the dimension. It appears that $b(q)$ is negative for

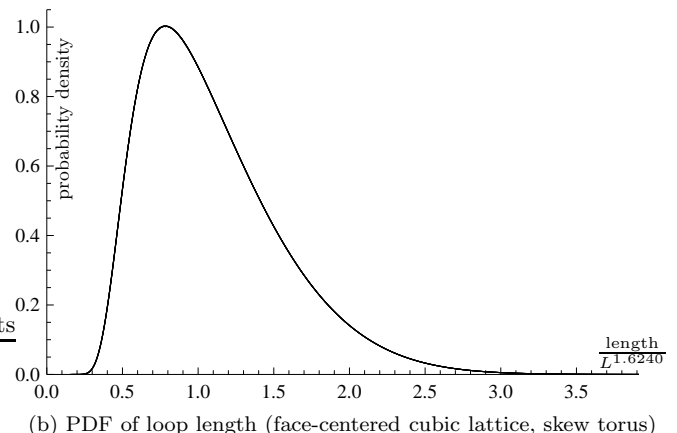
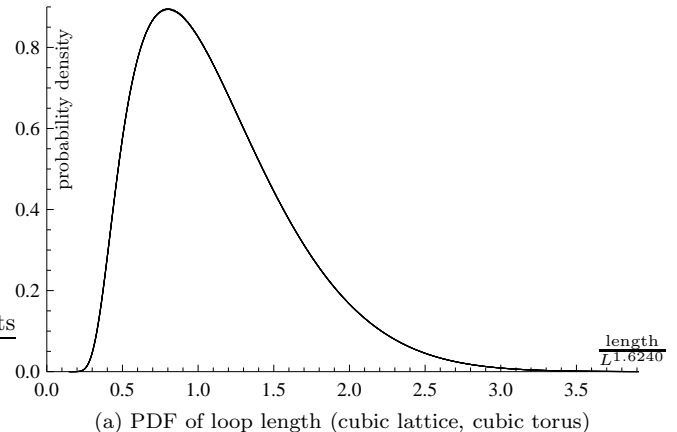
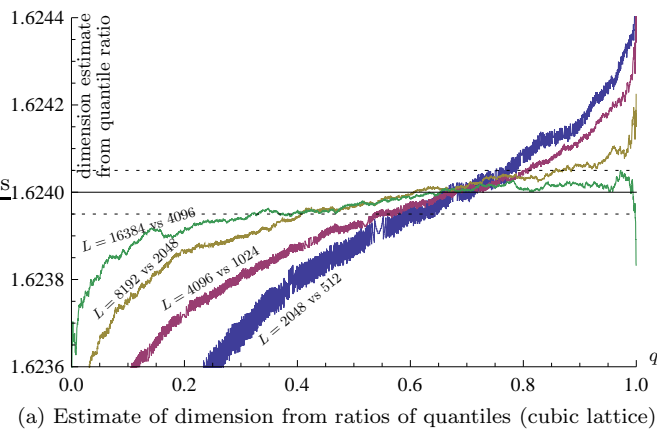
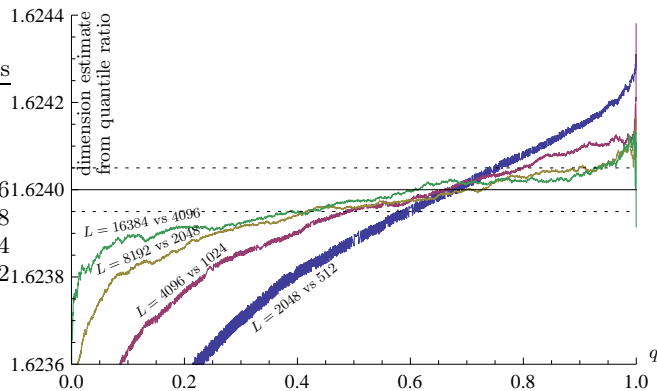


FIG. 1: Probability density function for the length of the loop-erased random loop on the $L \times L \times L$ cubic lattice (top) and face-centered cubic lattice (bottom). For both lattices, data is shown for $L = 2^9, 2^{10}, 2^{11}, 2^{12}, 2^{13}, 2^{14}$. For each L we effectively show a histogram of the loop lengths; the intervals are very short, but nonetheless contain many data points, so the histograms appear to be curves. Here the loop lengths have been scaled down by a factor of $L^{1.6240}$ to compare the data for different system sizes. At this scale, the curves for the six different L 's are indistinguishable, and appear to be one curve. The differences between the cubic and FCC curves arise because the FCC simulations were done on a skew torus.



(a) Estimate of dimension from ratios of quantiles (cubic lattice)



(b) Estimate of dimension from ratios of quantiles (FCC lattice)

FIG. 2: (Color online) Here we plot the quantile ratios $\log(Q_q(L)/Q_q(L/4))/\log(4)$ versus q for $L = 2^{11}, 2^{12}, 2^{13}, 2^{14}$ for the cubic lattice (top) and face-centered cubic lattice (bottom). The saw-tooth pattern, which is evident for $L = 2^{11}$ and still visible for $L = 2^{12}$, arises because the loop length is integer-valued. The saw teeth are more pronounced for the cubic lattice because it is bipartite. The curves for larger L become progressively more flat, and appear to be converging to a value in the range 1.62400 ± 0.00005 .

small q and positive for large q , taking the value 0 near $q = 0.7$. For this q the first correction term is 0, so the quantile ratios more precisely give z . The quantile ratios (as a function of q) appear to converge to a horizontal line at a geometric rate, in agreement with the formula. Additional analysis of the data suggests that the correction exponent $y - z$ is approximately in the range -0.8 to -0.85 . Based on these plots, together with the least-squares fits, we judge that the dimension z is likely to be 1.62400 ± 0.00005 .

TAIL BEHAVIOR

Also of interest are quantities such as the probability that a loop-erased path is unusually short. In two dimensions it was recently shown that the probability that a LERW path is shorter than λ times its expected

length decays exponentially fast in $\lambda^{-4/5+o(1)}$ (or faster) [26]. We estimated the corresponding tail behavior for 3D LERW, and found that it decays exponentially fast in $\lambda^{-\alpha}$ for α approximately 0.58 ± 0.02 . Perhaps the correct exponent α is the reciprocal of the dimension.

Acknowledgements. We thank Russ Lyons for comments on an earlier version.

- [1] S. N. Majumdar, Phys. Rev. Lett. **68**, 2329 (1992).
- [2] R. Pemantle, Ann. Probab. **19**, 1559 (1991).
- [3] D. B. Wilson, in *Proc. 28th ACM Symp. Theory of Computing* (ACM, 1996), pp. 296–303.
- [4] S. N. Majumdar and D. Dhar, Physica A **185**, 129 (1992).
- [5] V. B. Priezzhev, J. Stat. Phys. **98**, 667 (2000), cond-mat/9904054.
- [6] D. V. Kvitarev, S. Lübeck, P. Grassberger, and V. B. Priezzhev, Phys. Rev. E **61**, 81 (2000), cond-mat/9907157.
- [7] R. Kenyon, Acta Math. **185**, 239 (2000), math-ph/0011042.
- [8] R. Masson, Electron. J. Probab. **14**, no. 36, 1012 (2009), arXiv:0806.0357.
- [9] G. F. Lawler, O. Schramm, and W. Werner, Ann. Probab. **32**, 939 (2004), math/0112234v3.
- [10] G. F. Lawler, J. Fourier Anal. Appl. pp. 347–361 (1995).
- [11] G. Kozma, Acta Math. **199**, 29 (2007), math/0508344.
- [12] G. F. Lawler, in *Perplexing problems in probability* (Birkhäuser, 1999), Progr. Probab. #44, pp. 197–217.
- [13] A. J. Guttmann and R. J. Bursill, J. Stat. Phys. **59**, 1 (1990).
- [14] R. E. Bradley and S. Windwer, Phys. Rev. E **51**, 241 (1995).
- [15] L. Anton, Phys. Rev. Lett. **86**, 67 (2001), cond-mat/0002028.
- [16] H. Agrawal and D. Dhar, Phys. Rev. E **63**, 056115 (2001), cond-mat/0012102v1.
- [17] A. A. Fedorenko, P. L. Doussal, and K. J. Wiese, J. Stat. Phys **133**, 805 (2008), arXiv:0803.2357.
- [18] P. Grassberger, J. Stat. Phys. **136**, 399 (2009), arXiv:0905.3440.
- [19] B. Wieland and D. B. Wilson, Phys. Rev. E **68**, 056101 (2003), arXiv:1002.3220.
- [20] B. Duplantier, in *Les Houches, Session LXXXIII, 2005, Mathematical Statistical Physics* (Elsevier, 2006), pp. 101–217, math-ph/0608053.
- [21] D. Dhar and A. Dhar, Phys. Rev. E **55**, R2093 (1997), cond-mat/9704026.
- [22] R. Lyons, Y. Peres, and O. Schramm, Ann. Inst. H. Poincaré Probab. Statist. **39**, 779 (2003), math/0107.5055.
- [23] P. Hellekalek and S. Wegenkittl, ACM Trans. Model. Comput. Simul. **13**, 322 (2003).
- [24] P. L’Ecuyer and R. Simard, ACM Trans. Math. Software **33**, Art. 22, 40 (2007).
- [25] T. H. Cormen, C. E. Leiserson, R. L. Rivest, and C. Stein, *Introduction to algorithms* (MIT Press, 2009), 3rd ed.
- [26] M. T. Barlow and R. Masson (2009), arXiv:0910.5015.